

Modulation of Mesenchymal Stem Cell Shape in Enzyme-Sensitive Hydrogels Is Decoupled from Upregulation of Fibroblast Markers Under Cyclic Tension

Peter J. Yang, Ph.D.,¹ Marc E. Levenston, Ph.D.,² and Johnna S. Temenoff, Ph.D.³

Our laboratory has developed a tensile culture bioreactor as a system for understanding mesenchymal stem cell (MSC) differentiation toward a tendon/ligament fibroblast phenotype in response to cyclic tensile strain. In this study, we investigated whether increased degradability of the biomaterial carrier would induce changes in MSC morphology and subsequent upregulation of tendon/fibroblast markers under tensile strain. Degradability of a synthetic poly(ethylene glycol) hydrogel was introduced by incorporating either fast- or slow-degrading matrix metalloproteinase (MMP)-sensitive peptide sequences into the polymer backbone. Although a decline in cellularity was observed over culture in all sample groups, at 14 days, MSCs were significantly more spread in fast-cleaving gels ($84\% \pm 8\%$) compared with slow-cleaving gels ($59\% \pm 4\%$). Cyclic tensile strain upregulated tendon/ligament fibroblast-related genes, such as collagen III (3.8-fold vs. 2.1-fold in fast-degrading gels) and tenascin-C (2.5-fold vs. 1.7-fold in fast-degrading gels). However, few differences were observed in gene expression between different gel types. Immunostaining demonstrated increased collagen III deposition in dynamically strained gels at day 14, as well as increased collagen I and tenascin-C deposition at day 14 in all groups. Results suggest that cell spreading may not be a major factor controlling MSC response to cyclic strain in this system over 14 days. However, these findings provide key parameters for the design of future biomaterial carriers and strain regimens to prime stem cells to a tendon/ligament phenotype prior to release and use *in vivo*.

Introduction

IT HAS BEEN estimated that at least 200,000 people in the United States receive treatment for injuries to tendon or ligament tissue each year.¹ In response, a multitude of tissue engineering approaches have been employed to engineer replacement fibrous tissues.² Typically, either tendon/ligament fibroblasts or multipotent mesenchymal stem cells (MSCs) have been explored as cell sources for these constructs.³ MSCs offer an advantage in that they can be easily isolated and expanded to sufficient numbers for therapeutic use.⁴ For those utilizing MSCs as a cell source, a number of approaches employing culture under tensile strain to induce differentiation toward a fibroblastic lineage have been investigated.⁴⁻⁶ However, better model systems are needed to clarify the role that the biomaterial scaffold may play in affecting MSC response to external loading during the preculture (differentiation) period in order to optimize the preculture conditions for maximal cell differentiation.

In response, our laboratory has designed a well-controlled model system to better understand how changing the degradability of the extracellular environment will affect changes in cell morphology and subsequent differentiation under tensile loading. A previous study has shown that, in addition to tensile strain, substrate stiffness and cell geometry can affect cell fate.⁷ The regulation of cell shape and area has been implicated in driving MSC differentiation into either osteoblast or adipocyte lineages.^{8,9} For chondrogenic differentiation, a rounded shape has been shown to be highly linked with gene upregulation indicative of chondrogenesis.¹⁰ In engineering tendon/ligament tissues, changes in cell shape have been shown to affect collagen I and collagen III expression in anterior cruciate ligament cells seeded on blends of poly(caprolactone)/chitosan.¹¹ However, by using a primarily synthetic biomaterial with targeted degradation sites, such as that employed in this study, the local extracellular environment can be precisely tailored to enable cell

¹Wallace H. Coulter Department of Biomedical Engineering, Georgia Tech/Emory University, Atlanta, Georgia.

²Department of Mechanical Engineering, Stanford University, Stanford, California.

³Wallace H. Coulter Department of Biomedical Engineering, Institute for Bioengineering and Bioscience, Georgia Tech/Emory University, Atlanta, Georgia.

spreading in a highly controlled manner, facilitating examination of the interplay between cell shape and response to tensile strain.

To create this model system, poly(ethylene glycol) (PEG)-based synthetic hydrogels were chosen due to their cytocompatibility and the relative ease of tailoring these systems with specific functionalities.¹² In a previous work, PEG-based hydrogels were coupled with the adhesive peptide RGD and tensile strain to direct differentiation of MSCs toward a tendon/ligament fibroblast phenotype.⁵ MSCs demonstrated increased gene expression of collagen I, collagen III, and tenascin-C, as well as deposition of collagen I and tenascin-C after 21 days of culture. However, it is known that in traditional PEG-based gels, cells are unable to remodel their environment unless the polymer is specifically rendered degradable.¹³ Thus, to engineer susceptibility to cell-mediated degradation in these synthetic scaffolds, matrix metalloproteinase (MMP) cleavable sequences have been integrated into PEG-based hydrogels.^{14,15} MMPs are a family of endopeptidases that degrade extracellular matrix (ECM) components. These may be secreted by MSCs to cleave surrounding ECM and enable cell-initiated spreading, migration, and matrix deposition.^{12,16}

In this work, two different MMP-sensitive peptide sequences with comparatively slow or fast cleavage kinetics were incorporated into PEG hydrogels. These include the peptide sequence LGPA, derived from the collagen I $\alpha 1(I)$ peptide chain (slower degrading), and VPMSMRGG, derived from a combinatorial approach using a completely randomized dodecapeptide library and demonstrating enhanced susceptibility to MMP-1 and MMP-2 (faster degrading).^{14,15} In these studies, it was hypothesized that increasing enzyme susceptibility of the scaffolds would facilitate cell-mediated degradation of the local matrix, enabling changes in cell shape from spherical (round) to spread morphologies, while still maintaining the overall integrity of the cell-hydrogel construct, allowing for tensile loading over several weeks. Therefore, the objective of these studies was to characterize cell morphology in fast- and slow-degrading MMP-cleavable hydrogels, as well as use this model system to examine the effects of the resulting changes in cell morphology on MSC response to cyclic tensile strain in a custom-designed tensile culture bioreactor.

Methods

Oligo[poly(ethylene glycol)] fumarate and poly(ethylene glycol)-diacrylate polymer synthesis

Oligo[poly(ethylene glycol)] fumarate (OPF) (nominal molecular weight 10,000 Da) was synthesized as reported previously.⁵ Poly(ethylene glycol)-diacrylate (PEG-DA) was also synthesized according to published protocols¹⁷ using PEG with nominal molecular weight 3400 Da (Sigma-Aldrich). All polymers were stored at -20°C until further use. Gel permeation chromatography (GPC) was used to characterize the products (Styragel HR4E, Waters, LC-20AD; Shimadzu).

PEG-peptide synthesis

MMP-sensitive PEG products were synthesized according to published protocols.¹⁸ Slow-degrading (GGGLGPAGGK) and fast-degrading (GGVPMSMRGGGK) peptide sequences

(Aapptec) were dissolved in 50 mM sodium bicarbonate buffer at pH 8.5. Acrl-PEG-succinimidyl valerate (Acrl-PEG-SVA; $M_n \sim 3400$; Laysan Bio) was added at a molar ratio of 1:2.2 peptide:Acrl-PEG-SVA. After reacting for 3 h with gentle stirring, the mixed solution was transferred into 3500–5000 Da-molecular-weight cutoff dialysis tubing (Spectrum Labs) and dialyzed against distilled H_2O for 2 days to remove unreacted reagents. Similarly, GRGDS (PeproTech) was conjugated to Acrl-PEG-SVA as a cell-adhesive peptide targeting integrin binding. All three products, Acrl-PEG-GGGLGPAGGK-PEG-Acrl, Acrl-PEG-GGVPMSMRGGGK-PEG-Acrl, and Acrl-PEG-GRGDS were lyophilized (Labconco) and stored at -20°C .

Hydrogel degradation study

To test MMP-sensitive PEG hydrogel sensitivity to exogenous enzyme, hydrogels were fabricated and degraded as follows. Three polymers were tested: fast-degrading MMP-sensitive PEG, slow-degrading MMP-sensitive PEG, and a 50:50 wt% mixture of OPF 10K and PEG-DA (non-MMP-sensitive). Each polymer was dissolved in phosphate-buffered saline (PBS; pH 7.4) to create a 90 wt% water solution, and then sterile filtered using a $0.2\text{-}\mu\text{m}$ glass prefilter (Nalgene). About 0.07 wt% Irgacure 2959 (D2959; Ciba) in PBS/dimethyl sulfoxide was added to enable photopolymerization using UV light. Liquid prepolymer was deposited in autoclaved Teflon molds and exposed to UV light ($10.5\text{ mW}/\text{cm}^2$; 365 nm; UVP) for 10 min to fabricate 6 mm diameter \times 1 mm-thick gels. Gels were swollen in PBS at 37°C overnight and then deposited in sterile-filtered PBS with 4 mg/mL collagenase type II (Invitrogen). Gels in collagenase were then placed on a shaker plate shaking at $\sim 1\text{ Hz}$ at 37°C and monitored for degradation through the first 2 h, and then once every day thereafter. Collagenase solution was refreshed every 2 days. To characterize gels ($n=4$), fold swelling was calculated as previously described¹⁹ by W_w/W_d , where W_w is the wet weight of the hydrogel and W_d is the dry weight of the hydrogel.

Cell culture

Human MSCs were obtained from the Texas A&M Health Science Center College of Medicine Institute for Regenerative Medicine at Scott & White at passage 1. Cells were first thawed and plated in a single T-150 (Corning) for 24 h and then trypsinized and seeded in T-500 triple flasks (Nunc) at 50 cells/ cm^2 . The growth medium used was alpha minimum essential medium (α -MEM) with 16.3% fetal bovine serum (FBS), 1% antibiotic/antimycotic (Mediatech), and 4 mM L-glutamine (Mediatech). (Note: The FBS lot used was prescreened for MSC growth while maintaining collagen I, collagen III, and tenascin-C gene expression). Following expansion, cells were frozen at passage 2 in liquid nitrogen until further use. For these studies, cells from three separate donors were thawed, expanded as described, and combined prior to encapsulation at passage 3.

Cell encapsulation

Constructs for tensile culture were fabricated using slow-degrading and fast-degrading MMP-sensitive PEG using the formulation described previously. Acrl-PEG-GRGDS/

(1 $\mu\text{mol/g}$ swollen hydrogel) was added to enable cell adhesion. After solutions were filter sterilized, MSCs were added at 10×10^6 cells/mL and the hydrogel solution was deposited into Teflon molds as previously described to form gels $12.5 \times 9.5 \times 1.6$ mm.⁵ Following photo-crosslinking as described previously, tensile constructs were placed into six-well plates containing α -MEM with 10% FBS, 1% antibiotic/antimycotic, 4 mM L-glutamine, and 50 $\mu\text{g/mL}$ ascorbic acid (Sigma). Constructs were allowed to swell overnight to reach equilibrium swelling prior to culture as described below.

Tensile culture

Swollen fast-degrading and slow-degrading constructs with encapsulated MSCs were loaded into the tensile culture bioreactor and a loading regimen was applied for the duration of the experiment as reported previously.⁵ Specifically, constructs were maintained using 10% sinusoidal cyclic strain (5% offset, 5% amplitude) at 1 Hz for 3 h, followed by 3 h at 0% strain. Control hydrogels, both fast-degrading and slow-degrading constructs, were placed into a similar culture system and held at 0% strain. Culture medium was replaced every 2–3 days.

Cell viability and confocal imaging

At 1, 7, and 14 days, constructs ($n=3-4$) were removed from the bioreactor and incubated in LIVE/DEAD fluorescent staining solution (1 μM calcein AM and 1 μM ethidium homodimer-1 in PBS; Invitrogen) for 1 h and then imaged in PBS on a confocal microscope (Zeiss LSM 510). Images were taken every 10 μm through the entire thickness of the gel from three separate regions in each sample.

Image processing and particle analysis

Image files were processed using ImageJ 1.45h.²⁰ For circularity analysis, each image stack was smoothed using ImageJ's nearest neighbor function, and the green channel was isolated and thresholded using a cutoff of 60 (out of 255; threshold arbitrarily set). For each image, a particle analysis was performed to identify particles greater than 60 square pixels, and area (in μm^2), circularity, and a best fit ellipse were calculated for each particle in each image slice. Circularity is defined as $4\pi A/P^2$, where A and P are the area and perimeter of the particle. A perfect circle would have a circularity of 1; circularity decreases toward 0 in more elongated (spread) cells. To evaluate cells encapsulated within the interior of the gel, and to prevent single particles from being counted multiple times, five images—each 50 μm apart—were isolated from the middle portion of each image stack (defined as 200 μm away from the first and last image slices). This was performed in an automated fashion by automatically calculating a best-fit line in MATLAB (MathWorks) using a least squares regression and the average circularity of each slice within a stack. Five images were selected based on the best-fit line having a near-flat slope and a high goodness of fit. Particles were combined from multiple stacks (≥ 3 stacks per gel). To calculate particle alignment, the angle of the major axis of each best-fit ellipse was calculated relative to the x-axis of the image; 90° describes a particle oriented perpendicular to the x-axis. Histograms describing the distributions of particle circularity and angle

were normalized to the total number of particles in each sample (relative frequency) before plotting, so that the area under each curve is 1.

Cell number

At 1, 7, and 14 days, constructs ($n=7$) were removed from the tensile culture bioreactor and the wet weight of the hydrogel was measured. Gels were mechanically disrupted using a pellet grinder (VWR) and 500 μL distilled deionized water was added. To release DNA from encapsulated cells, samples were subjected to three repetitions of freeze-thaw cycles followed by sonication (Ultrasonik 28X; NEY). DNA content, representative of cell number, was determined by assaying the supernatant with PicoGreen reagents and included DNA standards (Invitrogen). Results were normalized against the hydrogel wet weight.

Gene expression

At 1, 7, and 14 days, constructs ($n=7$) were removed from the tensile culture bioreactor and processed using a pellet grinder as previously described. RNA was isolated from the disrupted hydrogels using QIAshredder columns (Qiagen), and RNA was purified using an RNeasy mini kit (Qiagen). cDNA was synthesized using SuperScript III reverse transcriptase (Invitrogen) and nucleotide mix (Promega). Real-time polymerase chain reaction (PCR) was performed using custom-designed primers, SYBR Green (Applied Biosystems), and a StepOnePlus™ Real-Time PCR System (Applied Biosystems). To analyze PCR amplification data, the raw fluorescence data were processed using LinRegPCR (v12.11; www.hartfaalcentrum.nl²¹). Genes examined included scleraxis, collagen I, collagen III, tenascin-C (days 1, 7, and 14), as well as tenomodulin, biglycan, and decorin (days 1 and 14), as markers for tendon/ligament fibroblast gene expression.^{4,22-25} Starting concentrations of each target gene were normalized to a geometric mean of three housekeeping genes—glyceraldehyde phosphate dehydrogenase, β -actin, and 18S ribosomal RNA.²⁶ Sequences for the forward and reverse primers used are listed in Table 1.

Histology and immunohistochemistry

At 1 and 14 days, samples ($n=2$) were removed from the tensile culture bioreactor and placed into a solution of 5% sucrose in PBS under vacuum. Over 2 h, the concentration was increased to 15% sucrose in three steps. Next, over 4 h, gels were subjected to 20% sucrose and gradually increasing concentrations of optimal cutting temperature compound (OCT; VWR) to achieve a 1:2 20% sucrose in PBS:OCT solution. After vacuum infiltration overnight, samples were frozen in liquid nitrogen and stored at -80°C . Infiltrated hydrogels were cryosectioned at 20 μm . Sections were fixed in acetone, blocked with 0.3% hydrogen peroxide in methanol, and then blocked with 1% bovine serum albumin solution with 2% goat serum and 0.1% Triton X-100. For primary antibody binding, sections were incubated overnight in mouse anti-human collagen I, collagen III, or tenascin-C at a concentration of 1:500 (Abcam). Sections were then rinsed in PBS and incubated for 30 min with goat polyclonal biotin-conjugated anti-mouse immunoglobulin G at 1:200 (Abcam), followed by signal amplification using an avidin-conjugated

TABLE 1. PRIMERS USED FOR REAL-TIME REVERSE TRANSCRIPTASE POLYMERASE CHAIN REACTION

Gene	Forward primer	Reverse primer
Biglycan	gccatgtggccctgtggcg	cccgaggtgtcagcgcccga
Collagen I	gaaaacatcccagccaagaa	gccagtctctatccatgt
Collagen III	tacggcaatcctgaactcc	gtgtgtttcgtgcaaccatc
Decorin	acagagcagcactaccctctctct	ggcctaggagggtcgaagtgcgggt
Scleraxis	gcgcgagcgagaccgaccaaca	cccggcagcagcagttgcc
Tenascin-C	ccacaatggcagatcctct	gttaacgcctgactgtggt
Tenomodulin	ccgctattgccgccgtctgtgaacc	gcgggccaccaccagttaaggca
GAPDH	gagtcaacggattgtgctgt	ttgatttggaggatctcg
18S rRNA	cgatggcgccgaaatagccttgc	cagtgtcttgggtgctggcctcg
β Actin	gcagtcggtggagcgagcatccc	tcccctgtgtgacttgggagaggac

Primers for collagen I, collagen III, GAPDH, and tenascin-C were developed from Doroski *et al.*⁵

horseradish peroxidase following manufacturer's protocols (Vectastain Elite ABC; Vector Laboratories). Finally, sections were exposed to diaminobenzidine chromogen (Abcam) following manufacturer's protocols for 4 min to generate color change. Three sections from each gel were examined. Negative controls were stained as described, but with the primary antibody omitted.

Statistics

Results are reported as mean \pm standard deviation. For statistical analysis, all data were first transformed using a Box-Cox transformation. Multifactor analysis of variances with Tukey's *post hoc* multiple comparison test was used to determine statistical significance with $p \leq 0.05$ to indicate significance between individual groups. For circularity, cell number, and gene expression analysis, the three factors were day, strain condition, and gel type. To analyze hydrogel degradation data, the two factors were day and sample. To determine possible trends in particle alignment, distributions of particle angles in individual gels were compared against a uniform angle distribution using chi-squared goodness-of-fit tests.

Results

Polymer synthesis and hydrogel degradation

From GPC results, the OPF used in the degradation study had M_n of $18,300 \pm 90$ with a polydispersity index of 4.8 ± 0.2 . PEG-DA had M_n of 3700 ± 20 and a polydispersity index of 1.1 ± 0.0 . All three types of hydrogels—nondegradable, slow-degrading, and fast-degrading—swelled in PBS overnight, with no differences between gel types after initial swelling (Fig. 1). Only one difference in fold swelling between non-degradable and fast-degrading gels in cell culture media was detected at day 1. No changes in fold swelling were noted at day 7. Upon gel exposure to collagenase, MMP-sensitive gels degraded rapidly; slow-degrading gels degraded in 1 h, while fast-degrading gels degraded in under 10 min (data not shown). In contrast, nondegradable gels remained unchanged in collagenase solution over 7 days.

Confocal microscopy and image analysis

As indicated by green staining visible in confocal microscopy, MSCs remained viable in both slow- and fast-degrading hydrogels, cultured statically or dynamically,

through 14 days of culture (Fig. 2). At day 1, MSCs were not visibly spreading in any gel type or strain condition, and this continued through day 7. However, at day 14, a certain amount of spreading was visually evident in all gels. No difference was seen between dynamically and statically cultured gels. Additionally, cell alignment was not visually apparent.

To differentiate between "spread" and "unspread" cells for particle analysis, a circularity < 0.65 was chosen to represent "spread" cells, based on average circularity values among all groups at day 1 (0.64 ± 0.02). Corroborating the qualitative examination of confocal microscopy images, few significant differences in the percentage of spread cells were found between day 1 and day 7 (Fig. 3a). Static fast-degrading gels on day 1 and dynamic fast-degrading gels on day 7 had more spread cells than slow-degrading groups. However, more cells were spread in fast-degrading gels at day 14, regardless of strain condition. Almost all day-14 groups also demonstrated significantly higher percentages of spread cells than their day 1 and 7 counterparts. To closely

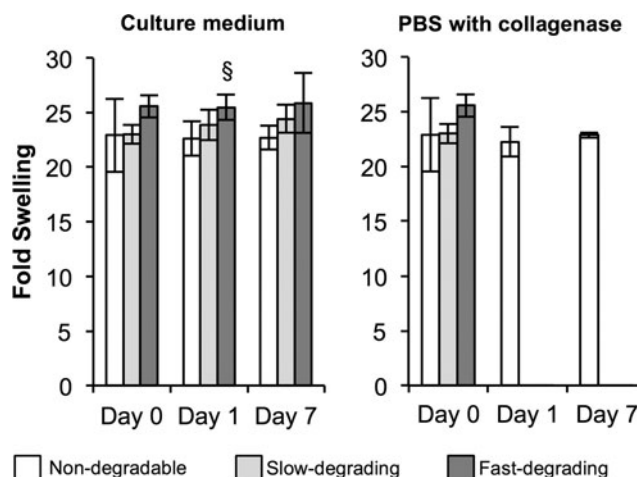


FIG. 1. Poly(ethylene glycol)-based hydrogels with collagenase-sensitive sequences exhibit similar swelling properties over time and degrade rapidly upon exposure to exogenous collagenase. Fold swelling of hydrogels in culture medium and in phosphate-buffered saline with collagenase solution at 0, 1, and 7 days. §Relative to nondegradable gel ($n = 4$; $p \leq 0.05$).

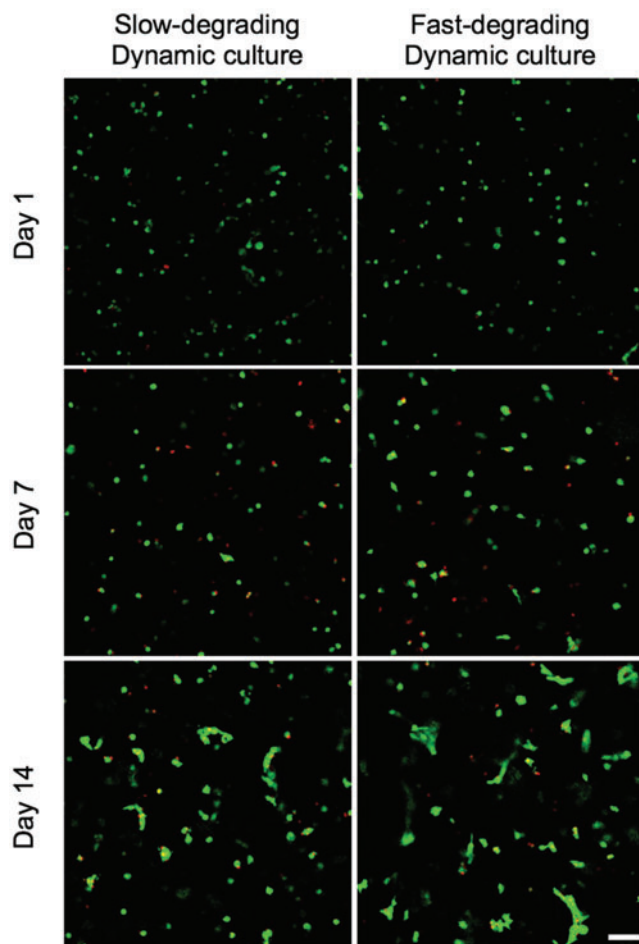


FIG. 2. hMSCs are viable and appear spread in both slow-degrading and fast-degrading gel types by day 14, regardless of culture condition. LIVE/DEAD images of encapsulated hMSCs ($n=3$) at 1, 7, and 14 days, cultured dynamically (Images taken from gels cultured statically appeared similar to images from dynamically cultured gels.). Scale bar: 100 μm . hMSC, human mesenchymal stem cell. Color images available online at www.liebertpub.com/tea

examine the differences between circularity distributions, histograms of circularity values were also calculated (Fig. 3b). At day 1, the circularity distribution trended toward a circularity of 1 (highly circular shape) in all groups. At day 14, some cells in slow-degrading gels had lower circularities; however, there was a more dramatic trend in fast-degrading gels toward low particle circularity.

Finally, particle alignment data were collected to determine whether cells had oriented in the direction of strain. There was no difference in average angle between any sample groups at any time point (data not shown). Angle distributions were plotted (Fig. 4). Visually, there were no notable differences in distribution between gel type, strain condition, or time. Chi-squared goodness-of-fit tests were used to qualitatively determine whether angle distributions in individual gels were nonuniform ($n=3-4$ per group). From this analysis, no statistical trends were evident between gel types or time points, suggesting there was no clear evidence of cell alignment over this period.

Cell number

DNA content/gel wet weight (indicative of cell number per gel) did not change between any groups at each time point (Fig. 5). However, all groups at days 14 and 7 were significantly lower than day 1 groups, indicating a decrease in DNA content (and therefore cell number) over time.

Gene expression

Scleraxis and tenomodulin gene expression were minimally expressed and amplified late as measured by PCR relative to housekeeping genes (data not shown). Scleraxis was maintained or downregulated over 14 days; static samples were downregulated at 14 days relative to day 1 samples, while dynamic samples were not different from day 1 (Fig. 6). Tenomodulin was largely maintained over 14 days, with only fast-degrading dynamic gels showing statistically significant downregulation relative to day 1 (Supplementary Fig. S1; Supplementary Data are available online at www.liebertpub.com/tea). Overall, collagen I mRNA expression either remained constant or downregulated over time; static samples at days 7 and 14 were significantly lower than day 1 samples, whereas dynamic samples were downregulated relative to day 7 but not significantly different from day 1. Statically cultured samples at day 7 were lower than their dynamically cultured counterparts.

In contrast, collagen III was upregulated in most sample types at day 7 relative to day 1 samples, and all collagen III expression levels in day 14 groups except the slow-degrading, static group were upregulated relative to their day 7 equivalents. In particular, there were significantly higher expression levels of collagen III in dynamically strained groups than statically cultured samples at day 14, regardless of gel type. Tenascin-C expression levels at day 7 were significantly upregulated in all groups relative to day 1 samples; however, tenascin-C gene expression levels in all day 14 groups except the fast-degrading dynamic group were downregulated relative to day 7. Nevertheless, expression levels of tenascin-C in all day 14 groups remained significantly upregulated relative to day 1, and there were also significant differences in tenascin-C expression noted between hydrogel types for each strain condition (static and dynamic). In particular, fast-degrading, dynamic groups at days 7 and 14 showed significantly lower tenascin-C expression relative to their slow-degrading counterparts.

Biglycan and decorin expression also demonstrated upregulation at day 14 (Supplementary Fig. S1). Specifically, biglycan showed a significant increase in expression between fast-degrading dynamic and fast-degrading static samples at day 14. Additionally, only dynamically cultured gels expressed increased biglycan levels at day 14 compared with day 1 samples. With decorin expression, all groups at day 14 were significantly higher than their day 1 counterparts; moreover, decorin expression was significantly higher in both fast-degrading and slow-degrading gels that had been dynamically cultured relative to their static controls at day 14. There were no differences at day 14 between gel types.

Histology

Immunohistochemistry revealed the presence of collagen I in all samples at day 1, with apparent increases in cell-

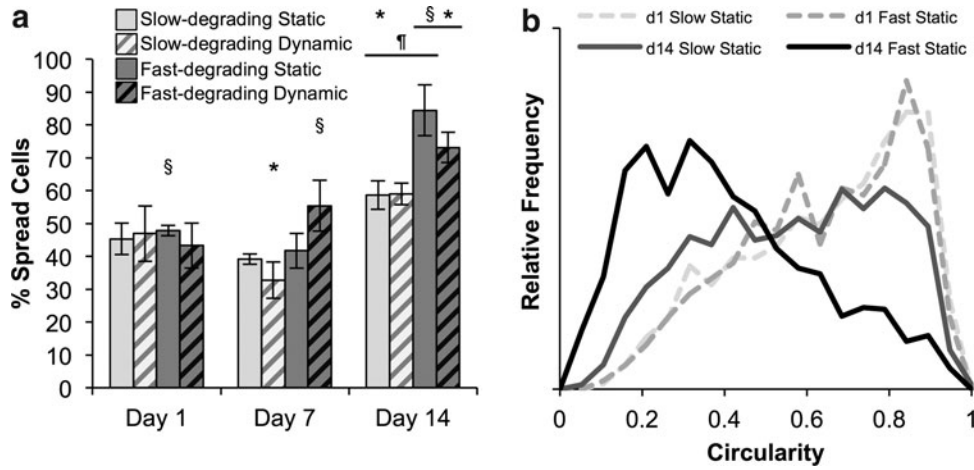


FIG. 3. Cells in slow- and fast-degrading gels spread over time, with significantly higher percentages of cells spread in fast-degrading gels versus slow-degrading gels at day 14. Strain condition appears to have no effect on cell spreading. **(a)** Percentage of spread cells (identified as having a circularity <0.65) in each gel type and culture condition at 1, 7, and 14 days. **(b)** Histograms of cell circularity distribution in representative statically cultured samples; curves are normalized so the area underneath each curve is 1. *Represents significance versus the same sample type on day 1; †versus the same sample type on day 7; §versus the other gel type at the same time point ($p < 0.05$).

associated deposition at day 14 (Fig. 7). The presence of collagen I did not appear to be different between static and dynamic samples. Cell-associated collagen III deposition was observed only at day 14, with more apparent staining in dynamically strained samples. Tenascin-C staining was seen at day 1 and continued through day 14; dynamically strained constructs seemed to show more prevalent staining overall. No cell-associated staining was observed in control sections that were not stained with primary antibody; however, some background staining was evident, especially in slow-degrading gels.

Discussion

In these experiments, hydrogels were fabricated using two established MMP-cleavable peptides with different MMP sensitivities and used to examine how degradability of the surrounding matrix affects MSC response to tensile strain.^{14,15} These sequences were specifically selected to maintain a similar hydrogel structure while tuning the overall degradability of the matrix, and have not previously been compared directly. As expected, all constructs remained

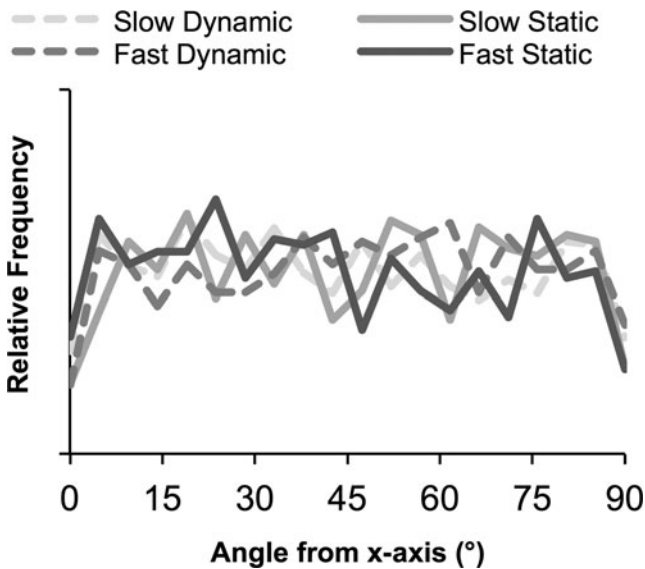


FIG. 4. No alignment was detected in sample groups at day 14. Histogram of particle alignment with x-axis from representative image stacks, normalized to total number of particles in each sample so the area under each curve is 1; 90° represents oriented perpendicular to the x-axis.

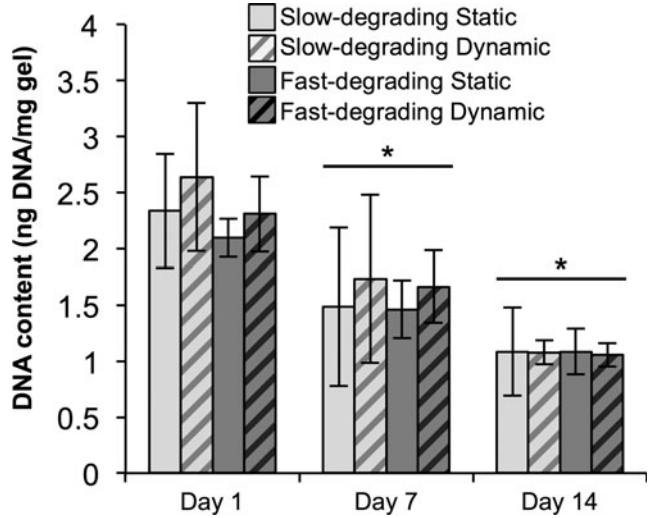


FIG. 5. There was no significant difference in DNA content between gel types or culture conditions, although DNA content decreased over time. PicoGreen data from encapsulated hMSCs ($n \geq 5$), cultured statically or dynamically, at days 1, 7, and 14. Data are normalized to gel wet weight. *Represents significance versus the same sample type at day 1 ($p < 0.05$).

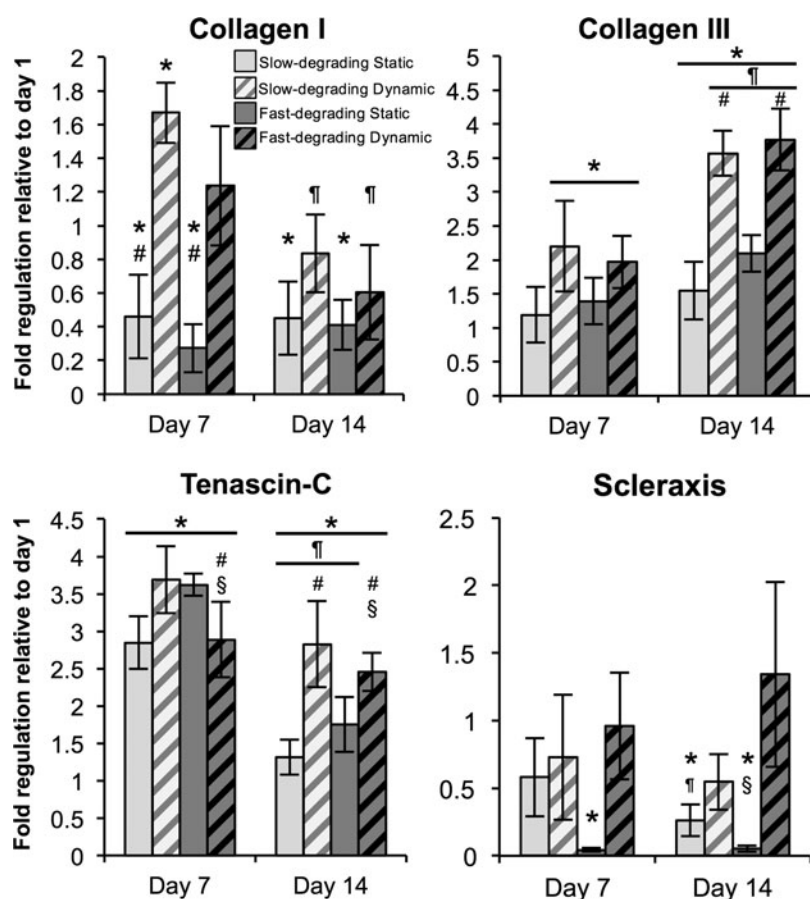


FIG. 6. Collagen III and tenascin-C, genes representative of tendon fibroblast differentiation, are significantly upregulated in dynamically cultured gels independent of gel type. Real-time polymerase chain reaction data of encapsulated hMSCs ($n \geq 5$), cultured statically or dynamically, at days 1, 7, and 14. Data are normalized to their respective day 1 groups. *Represents significance versus the same sample type at day 1; ¶versus the same sample type at day 7; #versus the other strain condition at the same time point; §versus the other gel type at the same time point ($p < 0.05$) (Note different y-axis scale for each graph).

intact over the culture period, allowing continued loading over 2 weeks *in vitro*.

Fabricated gels showed no statistically significant differences in fold swelling, implying that no differences exist in initial mesh size (and mechanical properties) between the two hydrogel types.^{27,28} However, gels rapidly degraded after exposure to collagenase. Moreover, enzyme-sensitive gels remained unchanged in culture medium over 1 week, demonstrating that active collagenase enzyme, and not other factors in medium, was the main effector of changes in hydrogel integrity. The implications of these results are two-fold: (1) cells should be able to locally degrade the gel by releasing MMPs, and (2) cells encapsulated within an MMP-sensitive hydrogel could be recovered, via addition of exogenous enzyme, for further analysis or implantation into tissue defects. Thus, this system allows cells to be exposed to highly controlled 3D environments, with precise biochemical and mechanical stimulation, to “prime” cells prior to retrieval for further therapeutic applications.

Confocal microscopy and image analysis were used in tandem to verify cell viability within the construct as well as evaluate changes in MSC morphology during culture. At 14 days, cell spreading was visually noted in both types of gels, with image analysis revealing that significantly more cells were spread in fast-degrading gels relative to slow-degrading gels, regardless of strain condition (Fig. 3). Although the exact proteases secreted by these MSCs were not characterized, enough active enzyme was produced to cleave local matrix and allow spreading to occur, as clearly evi-

denced in the LIVE/DEAD images (Fig. 2). The combination of the degradation and cell morphology results readily demonstrates that these synthetic hydrogel formulations enabled precise presentation of bioactive factors to encapsulated MSCs to control changes in cell shape over the culture period.

Although cells were able to spread in these scaffolds, no alignment was visually detected over time in dynamically or statically strained samples in any hydrogel type (Figs. 2 and 4). Previously, fibroblastic differentiation of stem cells was primarily examined in gels made of collagen (or other fibrous materials with comparatively large pore sizes), in which cells align in the direction of strain.²² In our studies, the presence of a covalently crosslinked, nonaligned scaffold may have deterred cell reorientation over this time period. However, it is possible that a PEG-based gel with larger pore sizes and sufficient proteolytic degradation will enable cell reorientation in response to strain.

PicoGreen data indicated that cell number in all groups decreased over time (Fig. 5). However, these results correlate with earlier work in our laboratory showing similar effects with MSCs encapsulated in nondegradable hydrogels.⁵ Importantly, no differences were noted in DNA content between gel types or strain conditions in this study, and confocal microscopy images demonstrated that cells were viable at all time points. Thus, cell number is likely not a driving factor behind differences seen among different gel types or strain conditions. Nevertheless, a decreasing cell number suggests that proliferation continues to be limited by a small hydrogel mesh size.²⁹ Future tailoring of these gels

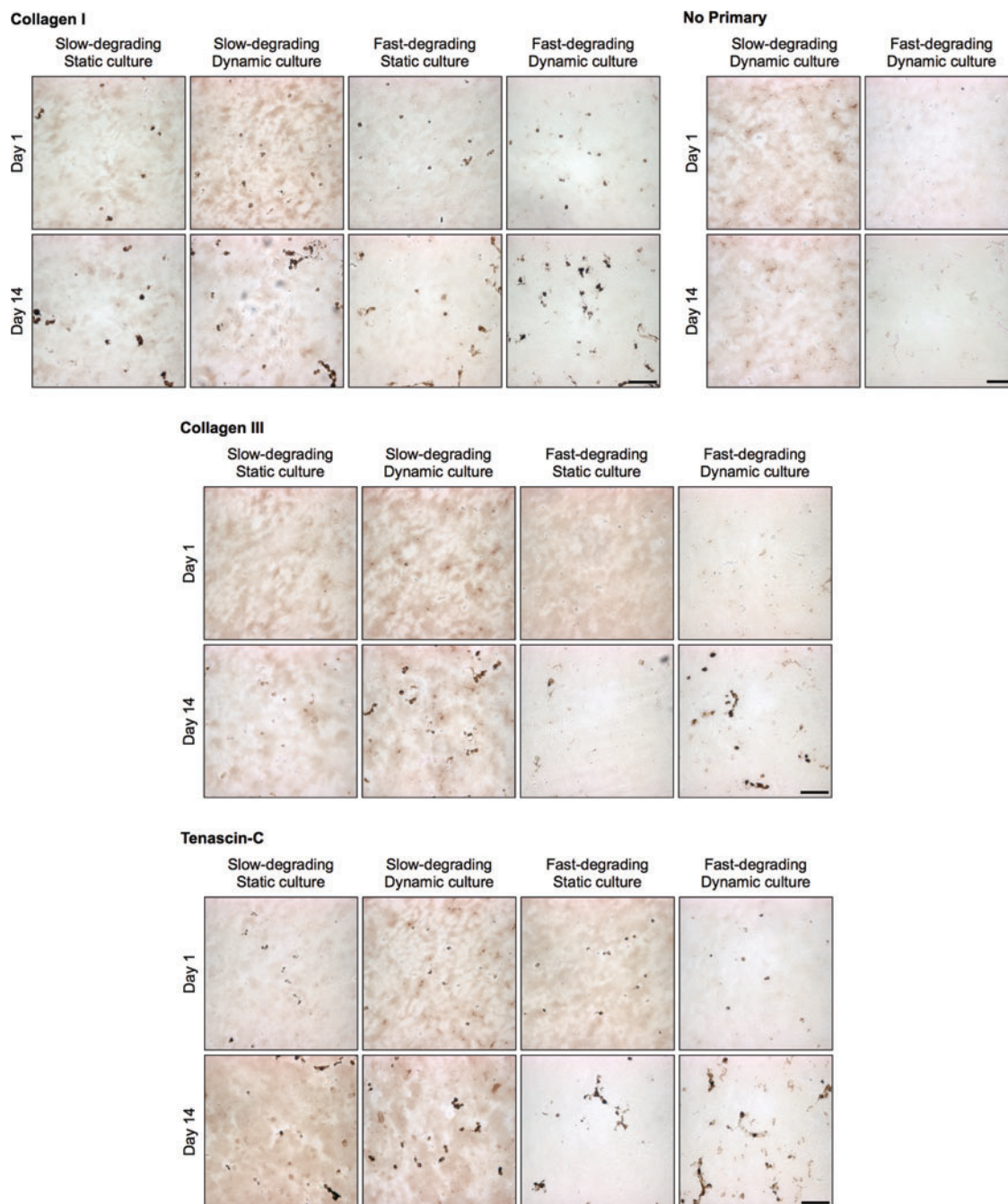


FIG. 7. MSCs encapsulated in both slow- and fast-degrading hydrogels demonstrate cell-associated collagen I, collagen III, and tenascin-C at 14 days, regardless of gel or culture type ($n=2$). Scale bar: 100 μm . Color images available online at www.liebertpub.com/tea

may include increasing pore size to provide space for cell proliferation in these materials while using other crosslinkers or reinforcement to maintain sufficient mechanical properties to allow for tensile loading of the constructs.

After loading for up to 14 days, MSCs embedded in both gel types were evaluated for expression of genes related to the tendon/ligament fibroblast phenotype (Fig. 6 and Supplementary Fig. S1). Time points in this study were selected based on previous work in our laboratory, and others, indicating that changes in gene expression and matrix deposition in response to tensile culture were observed after 7–14

days of tensile loading.^{5,30} Scleraxis, a transcription factor expressed by tendon progenitor cells in developing mesenchymal tissues, is often considered a tendon fibroblast marker.^{6,22} In this study, both scleraxis and tenomodulin, another tendon fibroblast marker,²³ was minimally expressed and was maintained or downregulated in all groups. In contrast, scleraxis expression was upregulated in a study using rat MSCs in a collagen gel using the same strain amplitude and rate, but with no rest period over 7 days.²² Another study utilizing primary human MSCs in collagen gels showed maintenance of scleraxis expression under 1%

strain at 1 Hz for 30 min/day over 7 days.⁶ Also, in a recent study, cells from a C3H10T1/2 MSC line in collagen gels upregulated scleraxis expression under 10% strain at 0.1 Hz with 10 s rest periods.³¹ Other work suggests that the binding substrate (in a 2D system) may affect differentiation as indicated by increases in scleraxis, tenomodulin, tenascin C, and collagen III expression by human MSCs on collagen-containing substrates over fibronectin-containing substrates.³² Tenomodulin expression appears to be also dependent on scleraxis expression.³³ Variations in scleraxis and tenomodulin expression from what was observed in this study may thus be attributable to differences in type of scaffold (collagen), cells, or strain regimen employed by other groups.

Contrary to some previously published reports,^{6,22} collagen I gene expression was downregulated over time in all gels, and although minor differences were shown between static and dynamic gels at day 7, this difference was not evident at day 14. These results differ from previous results in our laboratory using the same strain regimen, although those experiments used a scaffold that was not enzyme-degradable and MSCs from a different cell bank. The reason for the downregulation is unclear, although one report suggests that some changes in gene expression are dependent on scaffold and cell orientation.³⁴ Since no orientation was observed in these gels, the lack of directional bias may have inhibited potential changes to collagen I expression. However, other results using bone-marrow-derived MSCs in a collagen scaffold have indicated that collagen I remains relatively unchanged under strain.⁶ From immunostained sections, collagen I deposition was detected at day 1 and more intense staining was observed at day 14, regardless of gel and strain parameters. The deposition observed may simply be a reflection of a high resident level of gene expression observed at day 1 relative to other tested genes (data not shown); therefore, additional gene upregulation might not be expected in this system.

Collagen III and tenascin-C are frequently used as markers of tendon/ligament fibroblast differentiation.^{4,5,35,36} Dynamically strained samples, regardless of gel type, demonstrated an increase in collagen III expression, both over time and relative to static samples. Correspondingly, immunostaining revealed collagen III staining only in dynamically strained gels. This correlates well with data from our laboratory and other studies, where collagen III has been identified as part of the native tendon repair process.^{5,37,38} Tenascin-C levels in all gels at days 7 and 14 were upregulated relative to day 1, with generally higher expression at day 7 relative to day 14. Importantly, however, dynamic samples exhibited significantly higher expression levels of tenascin-C relative to static samples on day 14. Tenascin-C has been previously shown to be regulated by mechanical strain³⁹ but has also been speculated to play an "inhibitory for spreading" role that allows cells to modify adhesion contacts to avoid overstretching.⁴⁰ Thus, restricting the ability to alter cell shape under strain may have triggered increased tenascin-C expression in slow-degrading dynamic gels relative to fast-degrading dynamic gels on days 7 and 14. Differences in gene expression levels, however, were not readily correlated with immunostaining. Tenascin-C was detected at days 1 and 14, with visually increased staining in all samples at day 14. The lack of differences between groups

at day 14 may have been related to the consistent expression levels between groups on day 7. Longer culture times might provide tensile-strain-related upregulation of gene expression more time to emerge in the form of increased staining at time points beyond day 14.

Biglycan and decorin are also used as markers of tendon/ligament fibroblast differentiation and are constitutively found in tendon tissues.^{24,25,41} In our studies, decorin showed significant upregulation of all samples at day 14, with significantly higher expression in dynamic than in static samples at day 14 (Supplementary Fig. S1). Biglycan also demonstrated significantly higher expression in the dynamic than static samples at day 14 only in fast-degrading samples. These results indicate expression of other tendon-related markers and further support the ability of this system to induce differentiation toward a tendon/ligament fibroblast phenotype.

In this work, synthetic, "blank slate" materials were used to present bioactive factors and modulate degradability and hydrogel properties in a precisely controlled manner to investigate the specific role of biomaterial degradation on changes in cell morphology and response to applied cyclic tensile strain. In particular, the responses of cells to tensile strain when encapsulated in gels of different MMP sensitivities have not been previously examined. Together, the results of this study suggest that, within the range of scaffold degradability that could be engineered into this system and still allow for long-term loading, hydrogel susceptibility to MMP degradation, with corresponding changes in morphology of embedded cells, did not affect MSC response to cyclic tensile strain over 14 days. While this result was unexpected, it should be noted that, in these experiments, significant cell spreading was seen only at 14 days, so a longer culture period may be needed to allow changes in spreading to affect gene expression levels accordingly. It is also possible that the inclusion of RGD peptides, which interact with integrins on MSCs in both gel types, might facilitate cytoskeletal interactions with the synthetic scaffold and enable sensing of mechanical strain.⁴² In addition, the specific integrin ligands bound may also play a role in the differentiation response,³² so future work may explore the role of engaging specific integrins in combination with changes in morphology on response to strain in this system. Finally, other aspects of the local mechanical environment, including changes in fluid flow, may change due to strain, the extent of local degradation, and possible pericellular matrix deposited by cells over time, subsequently affecting cytoskeletal organization and enabling MSCs in slow-degrading gels to respond to tensile strain even if their ability to spread is limited.⁴³

Conclusions

The experiments described here demonstrate that incorporation of differentially degradable peptide sequences in a synthetic hydrogel impacted the morphology of embedded MSCs while maintaining sufficient mechanical integrity to allow long-term mechanical loading of cell-hydrogel constructs. Moreover, MSCs encapsulated in MMP-sensitive PEG-based gels reacted to tensile strain through upregulation of collagen III, tenascin C, and decorin, which are ECM molecules associated with the tendon/ligament fibroblast

phenotype. However, little difference in response to tensile strain from cells embedded in either slow- or fast-degrading gels was observed. Such results suggests that in these degradable, synthetic hydrogel systems spreading may not be a major factor controlling MSC response to cyclic strain, at least over this time period. However, these findings further support this system as a well-controlled platform that allows exploration of the effects of material formulation on resulting cell response to exogenous cues, such as mechanical loading, without confounding effects from the use of a material with other inherent bioactivity. As such, these experiments contribute key parameters toward the design of future biomaterial carriers and strain regimens to prime stem cells to a tendon/ligament phenotype prior to release and use *in vivo*.

Acknowledgments

The authors thank Taymour Hammoudi (Temenoff Lab) for developing the cryopreservation technique used for histology. This work was supported by NIH R21 EB8918, and an NSF Graduate Research Fellowship to P.J.Y. Some of the materials employed in this work were provided by the Texas A&M Health Science Center College of Medicine Institute for Regenerative Medicine at Scott & White through a grant from NCRP of the NIH, Grant #P40RR017447.

Disclosure Statement

No competing financial interests exist.

References

- Pennisi, E. Tending tender tendons. *Science* **295**, 1011, 2002.
- Yang, P.J., and Temenoff, J.S. Engineering orthopedic tissue interfaces. *Tissue Eng Part B Rev* **15**, 127, 2009.
- Butler, D.L., Juncosa-Melvin, N., Boivin, G.P., Galloway, M.T., Shearn, J.T., Gooch, C., *et al.* Functional tissue engineering for tendon repair: a multidisciplinary strategy using mesenchymal stem cells, bioscaffolds, and mechanical stimulation. *J Orthop Res* **26**, 1, 2008.
- Vunjak-Novakovic, G., Altman, G., Horan, R., and Kaplan, D.L. Tissue engineering of ligaments. *Annu Rev Biomed Eng* **6**, 131, 2004.
- Doroski, D.M., Levenston, M.E., and Temenoff, J.S. Cyclic tensile culture promotes fibroblastic differentiation of marrow stromal cells encapsulated in poly(ethylene glycol)-based hydrogels. *Tissue Eng Part A* **16**, 3457, 2010.
- Kuo, C.K., and Tuan, R.S. Mechanoactive tenogenic differentiation of human mesenchymal stem cells. *Tissue Eng Part A* **14**, 1615, 2008.
- Engler, A.J., Sen, S., Sweeney, H.L., and Discher, D.E. Matrix elasticity directs stem cell lineage specification. *Cell* **126**, 677, 2006.
- Kilian, K.A., Bugarija, B., Lahn, B.T., and Mrksich, M. Geometric cues for directing the differentiation of mesenchymal stem cells. *Proc Natl Acad Sci U S A* **107**, 4872, 2010.
- McBeath, R., Pirone, D.M., Nelson, C.M., Bhadriraju, K., and Chen, C.S. Cell shape, cytoskeletal tension, and RhoA regulate stem cell lineage commitment. *Dev Cell* **6**, 483, 2004.
- Woods, A., Wang, G., and Beier, F. RhoA/ROCK signaling regulates Sox9 expression and actin organization during chondrogenesis. *J Biol Chem* **280**, 11626, 2005.
- Shao, H.-J., Lee, Y.-T., Chen, C.-S., Wang, J.-H., and Young, T.-H. Modulation of gene expression and collagen production of anterior cruciate ligament cells through cell shape changes on polycaprolactone/chitosan blends. *Biomaterials* **31**, 4695, 2010.
- Lutolf, M.P., and Hubbell, J.A. Synthetic biomaterials as instructive extracellular microenvironments for morphogenesis in tissue engineering. *Nat Biotechnol* **23**, 47, 2005.
- Kloxin, A.M., Kloxin, C.J., Bowman, C.N., and Anseth, K.S. Mechanical properties of cellularly responsive hydrogels and their experimental determination. *Adv Mater* **22**, 3484, 2010.
- West, J., and Hubbell, J. Polymeric biomaterials with degradation sites for proteases involved in cell migration. *Macromolecules* **32**, 241, 1999.
- Patterson, J., and Hubbell, J.A. Enhanced proteolytic degradation of molecularly engineered PEG hydrogels in response to MMP-1 and MMP-2. *Biomaterials* **31**, 7836, 2010.
- Mannello, F., Tonti, G.A.M., Bagnara, G.P., and Papa, S. Role and function of matrix metalloproteinases in the differentiation and biological characterization of mesenchymal stem cells. *Stem Cells* **24**, 475, 2006.
- Patel, D., Menon, R., and Taite, L.J. Self-assembly of elastin-based peptides into the ECM: the importance of integrins and the elastin binding protein in elastic fiber assembly. *Biomacromolecules* **12**, 432, 2011.
- Moon, J.J., Saik, J.E., Poché, R.A., Leslie-Barbick, J.E., Lee S-H, Smith, A.A., *et al.* Biomimetic hydrogels with pro-angiogenic properties. *Biomaterials* **31**, 3840, 2010.
- Qiu, Y., Lim, J.J., Scott, L., Adams, R.C., Bui, H.T., and Temenoff, J.S. PEG-based hydrogels with tunable degradation characteristics to control delivery of marrow stromal cells for tendon overuse injuries. *Acta Biomater* **7**, 959, 2011.
- Abramoff, M.D., Magalhaes, P.J., and Ram, S.J. Image processing with ImageJ. *Biophotonics Int* **11**, 36, 2004.
- Ruijter, J.M., Ramakers, C., Hoogaars, W.M.H., Karlen, Y., Bakker, O., van den Hoff, M.J.B., *et al.* Amplification efficiency: linking baseline and bias in the analysis of quantitative PCR data. *Nucleic Acids Res* **37**, e45, 2009.
- Thomopoulos, S., Das, R., Birman, V., Smith, L., Ku, K., Elson, E.L., *et al.* Fibrocartilage tissue engineering: the role of the stress environment on cell morphology and matrix expression. *Tissue Eng Part A* **17**, 1039, 2011.
- Jelinsky, S.A., Archambault, J., Li, L., and Seeherman, H. Tendon-selective genes identified from rat and human musculoskeletal tissues. *J Orthop Res* **28**, 289, 2010.
- Schneider, P.R.A., Buhmann, C., Mobasher, A., Matis, U., and Shakibaei, M. Three-dimensional high-density coculture with primary tenocytes induces tenogenic differentiation in mesenchymal stem cells. *J Orthop Res* **29**, 1351, 2011.
- Bi, Y., Ehrlich, D., Kilts, T.M., Inkson, C.A., Embree, M.C., Sonoyama, W., *et al.* Identification of tendon stem/progenitor cells and the role of the extracellular matrix in their niche. *Nat Med* **13**, 1219, 2007.
- Vandesompele, J., De Preter, K., Pattyn, F., Poppe, B., Van Roy, N., De Paep, A., *et al.* Accurate normalization of real-time quantitative RT-PCR data by geometric averaging of multiple internal control genes. *Genome Biol* **3**, RESEARCH0034, 2002.
- Temenoff, J.S., Athanasiou, K.A., LeBaron, R.G., and Mikos, A.G. Effect of poly(ethylene glycol) molecular weight on tensile and swelling properties of oligo(poly(ethylene glycol) fumarate) hydrogels for cartilage tissue engineering. *J Biomed Mater Res Part A* **59**, 429, 2002.
- Durst, C.A., Cuchiara, M.P., Mansfield, E.G., West, J.L., and Grande-Allen, K.J. Flexural characterization of cell encapsulated PEGDA hydrogels with applications for tissue engineered heart valves. *Acta Biomater* **7**, 2467, 2011.

29. Bott, K., Upton, Z., Schrobback, K., Ehrbar, M., Hubbell, J.A., Lutolf, M.P., *et al.* The effect of matrix characteristics on fibroblast proliferation in 3D gels. *Biomaterials* **31**, 8454, 2010.
30. Connelly, J.T., Vanderploeg, E.J., Mouw, J.K., Wilson, C.G., and Levenston, M.E. Tensile loading modulates bone marrow stromal cell differentiation and the development of engineered fibrocartilage constructs. *Tissue Eng Part A* **16**, 1913, 2010.
31. Scott, A., Danielson, P., Abraham, T., Fong, G., Sampaio, A.V., and Underhill, T.M. Mechanical force modulates scleraxis expression in bioartificial tendons. *J Musculoskeletal Neuronal Interact* **11**, 124, 2011.
32. Sharma, R.L., and Snedeker, J.G. Biochemical and biomechanical gradients for directed bone marrow stromal cell differentiation toward tendon and bone. *Biomaterials* **31**, 7695, 2010.
33. Shukunami, C., Takimoto, A., Oro, M., and Hiraki, Y. Scleraxis positively regulates the expression of tenomodulin, a differentiation marker of tenocytes. *Dev Biol* **298**, 234, 2006.
34. Heo, S.-J., Nerurkar, N.L., Baker, B.M., Shin, J.-W., Elliott, D.M., and Mauck, R.L. Fiber stretch and reorientation modulates mesenchymal stem cell morphology and fibrous gene expression on oriented nanofibrous microenvironments. *Ann Biomed Eng* **39**, 2780, 2011.
35. Hankemeier, S., Keus, M., Zeichen, J., Jagodzinski, M., Barkhausen, T., Bosch, U., *et al.* Modulation of proliferation and differentiation of human bone marrow stromal cells by fibroblast growth factor 2: potential implications for tissue engineering of tendons and ligaments. *Tissue Eng* **11**, 41, 2005.
36. Fan, H., Liu, H., Wong, E.J.W., Toh, S.L., and Goh, J.C.H. *In vivo* study of anterior cruciate ligament regeneration using mesenchymal stem cells and silk scaffold. *Biomaterials* **29**, 3324, 2008.
37. Lin, T.W., Cardenas, L., and Soslowsky, L.J. Biomechanics of tendon injury and repair. *J Biomech* **37**, 865, 2004.
38. Maffulli, N., Ewen, S.W., Waterston, S.W., Reaper, J., and Barrass, V. Tenocytes from ruptured and tendinopathic achilles tendons produce greater quantities of type III collagen than tenocytes from normal achilles tendons. An *in vitro* model of human tendon healing. *Am J Sports Med* **28**, 499, 2000.
39. Maier, S., Lutz, R., Gelman, L., Sarasa-Renedo, A., Schenk, S., Grashoff, C., *et al.* Tenascin-C induction by cyclic strain requires integrin-linked kinase. *Biochim Biophys Acta* **1783**, 1150, 2008.
40. Chiquet-Ehrismann, R., and Chiquet, M. Tenascins: regulation and putative functions during pathological stress. *J Pathol* **200**, 488, 2003.
41. Rees, S.G., Dent, C.M., and Caterson, B. Metabolism of proteoglycans in tendon. *Scand J Med Sci Sports* **19**, 470, 2009.
42. Hersel, U., Dahmen, C., and Kessler, H. Rgd modified polymers: biomaterials for stimulated cell adhesion and beyond. *Biomaterials* **24**, 4385, 2003.
43. Lavagnino, M., Arnoczky, S.P., Kepich, E., Caballero, O., and Haut, R.C. A finite element model predicts the mechanotransduction response of tendon cells to cyclic tensile loading. *Biomech Model Mechanobiol* **7**, 405, 2008.

Address correspondence to:

Johnna S. Temenoff, Ph.D.

Wallace H. Coulter Department of Biomedical Engineering

Institute for Bioengineering and Bioscience

Georgia Tech/Emory University

313 Ferst Drive

Atlanta, GA 30332

E-mail: johnna.temenoff@bme.gatech.edu

Received: December 22, 2011

Accepted: June 13, 2012

Online Publication Date: July 24, 2012